Antimicrobial Activity of Alloy Metals and Phage on *Elizabethkingia anophelis*

Dora Gadung Dawat[1], Asdren Zajmi[1*], Safaa Najah Saud[2]

[1]Department of Diagnostic and Allied Health Science, Faculty of Health and Life Sciences, Management and Science University, 40100 Shah Alam, Selangor, Malaysia.

[2]Department of Engineering & Technology, Faculty of Information Sciences and Engineering, Management and Science University, 40100 Shah Alam, Selangor, Malaysia.

Abstract

Elizabethkingia anophelis is an emerging opportunistic pathogen transmitted via the *Anophelis gambiae* mosquito. It is associated with a high mortality rate due to its resistance to multiple antibiotics, including multiple beta-lactamases and efflux system. The aim of this study is to isolate phages capable of killing *E. anophelis* and the combination of phage with seven types of alloy metals (titanium (Ti), tantalum (Ta), titanium-tantalum (Ti-Ta), silver (Ag), titanium-tantalum-silver (Ti-Ta-Ag), niobium (Nb) and graphene nano-oxide (Go)) against *E. anophelis*. For the isolation of bacteriophages, water samples were collected from a sewage. Seven types of alloy metals were evaluated for their antibacterial and synergistic activities using the disc diffusion method followed by microdilution broth. The plaques were then isolated and combined with each of the seven alloy metals for standard double layer agar. Plaque morphologies were observed and shown to be clear and irregular. The highest mean of inhibition zone was demonstrated by Ta-Ti, with a value of 20.00±5.19 mm followed by Ti 12.00±2.64 mm, Go 11.00±1.00 mm, Ta 10.33±1.52 mm, Nb 9.33±0.57 mm, Ag 8.66±0.57 mm, and TiTa-Ag 8.66±1.15 mm. As for minimum inhibitory concentration (MIC), all seven alloy metals were shown to have restrained the growth of tested *E. anophelis* in the range of 25 to 400 mg/mL, whereas the minimum bactericidal concentration showed a restrain in the growth of the tested *E. anophelis* in the range of 50 to 400mg/mL. However, in regard the combination of the phage and alloy metals, the nanoparticles showed no significant activity. Hence, these findings conclude that both phage and alloy metals are better used independently than when combined.

Keywords: *Elizabethkingia anophelis*, Bacteriophage, *Anophelis gambiae*, antibiotic resistance, alloy metals.

Article Info

Received 2nd November 2020
Accepted 1st February 2021
Published 1st April 2021
*Corresponding author: Asdren Zajmi; email: asdren_zajmi@msu.edu.my

ISSN: 1823-7010, eISSN: 2600-7444

Introduction

Elizabethkingia anophelis is a Gram-negative, aerobic, non-motile, rod-shaped bacterium, oxidase (+), indole (+), catalase (+) and ONPG- positive, and belongs to the family *Flavobacteriaceae* [1]. The bacterium has two growth optima at 30-31°C and 37°C [2]. It is an emerging, opportunistic, and nosocomial pathogen. Neonates, post-surgery patients or old people with underlying diseases are most susceptible to *E. anophelis* infection [3].

According to Janda and Lopez [1] , the primary infection associated with *E. anophelis* have been cases of meningitis or sepsis in the very young (premature, neonates) or in adults with underlying medical conditions. *E. anophelis* is an emerging opportunistic pathogen, and this infection is associated with a high mortality rate due to its resistance to multiple antibiotics, including multiple beta-lactamases and efflux system [4].

This bacterium has been discovered in the midgut of the malaria vector mosquito *Anophelis gambiae* in 2011 and soon after, it was reported as the cause of neonatal meningitis in the Central African Republic. It has also been increasingly reported to cause outbreaks in Hong Kong**,** Taiwan, and a nosocomial outbreak in an intensive-care unit in Singapore [5-7]. Recently, a multistate cluster of *E. anophelis* infection was isolated from dozens of patients reported in the Midwestern United States and these infections were associated with significant morbidity and mortality [8]. In addition, an unusual case of *E. anophelis* meningitis was also reported in a Danish male who had a travel history to Malaysia 7 weeks prior to hospitalization [9]. *E. anophelis* has been reported as dominant *Elizabethkingia* species in Singapore [7] in comparison with Malaysia where we have more reports of *Elizabethkingia meningoseptica* [10-12]. There is a very close resemblance between *Elizabethkingia* species, thus this has led to *E. anophelis frequently* being misdiagnosed as *E. meningoseptica* via routine phenotypic and biochemical test with automated microbial identification systems [3].

In fact, in all previously reported clinical cases by Lau et al. [5], *E. anophelis* isolates were resistant to most antibiotics recommended for empirical therapy, including third generation cephalosporins, aminoglycosides, and carbapenems. Most of this bacterium genomes consistently harbour multi-drug resistance genes; this includes the two metallo-beta-lactamase genes *bla*GOB and *blaBla*B associated with resistance to carbapenems [13]. Carbapenems are often used as the ‘’last-resort antibiotics’’ or ‘’last-line drugs’’ when patients with infectious diseases become gravely ill or are suspected of harbouring resistant bacteria. Carbapenems play a critical role in the armament of antibiotics. Among many of β-lactams, carbapenems have the broadest spectrum of activity and the greatest potential against Gram-positive as well as Gram-negative bacteria [14]. Therefore, *E. anophelis* infection should be considered a clinically significant problem and the investigation of antibiotic resistance mechanisms is warranted [13].

This study aimed at investigating alternative treatment options for multidrug-resistant bacterial infections by combining bacteriophage with different alloy metals. The bacteriophage can lyse the bacterial cell with specificity. This phage therapy is also non-toxic to the human body, where it only infected the specific bacteria [15]. As for metal powders, it has a nanoparticle which acts as antimicrobial properties that inhibiting bacterial growth. Unlike antibiotics, the mode of action is direct contact with the bacterial cell wall, without penetrating the cell. This rise the promising that Nanoparticles will be less likely to promote resistance in bacteria in comparison to antibiotics. Hence, this combination of phage and alloy metals could help in decreasing the incidents of nosocomial infection.

Materials and Methods

Sample Preparation for Bacteria

The bacteria host, *Elizabethkingia anophelis* (NCTC13869) was obtained from the National Collection of Type Cultures (NTCC) in a freeze-dried suspension form, supplied in a glass ampule sealed under vacuum. It was re-isolated in tryptone soy broth (TSB) and culture on tryptone soy agar (TSA) and was incubated at 37°C for 24 hours. After the incubation at 37°C, the cultured tryptone soy broth (TSB) was stored in 4°C.

Isolation of Phage Sample

Crude sewage water was obtained from Seksyen 2, Shah Alam. The sewage water was then transferred into a 15 mL sterile centrifuge and underwent centrifugation at 20,000 rpm for 10 minutes [16]. The supernatant was double filtered through a 0.45 μm pore sized and then followed by filtration within a 0.22 μm sterile pore sized to attain the phage sample. The phage sample was then stored in the dark at 4^{O}C in SM buffer that had been prepared [17].

Alloy Metals Dilution Preparation

A 200 mg of listed metal powders (Table 1) were diluted separately with 900μL of distilled water and 10% of DMSO. For the disc diffusion method, 200 mg of Graphene Oxide (GO) and Niobium (Nb) was diluted with 1000μL of distilled water. A 400 mg/mL of Titanium, Tantalum, Silver, Titanium-Tantalum, Titanium-Tantalum-Silver, Graphene Oxide and Niobium powder was prepared for MIC and MBC.

Table 1. Used powder specifications

GROUP	POWDER	CONCENTRATION (WT.%)	PURITY (%)	SIZE (μM)
GROUP A	*Titanium (Ti)*	*100*	*99.99*	*45*
	Tantalum (Ta)	*100*	*99.999*	*45*
	Silver (Ag)	*100*	*99.99*	*45*
	Titanium-Tantalum	$Ti_{57wt.\%}$-$Ta_{43wt.\%}$	……	……
	Titanium-Tantalum-Silver	$Ti_{55wt.\%}$-$Ta_{43wt.\%}$-$Ag_{2wt.\%}$	……	……
GROUP B	*Graphene Oxide (GO)*	*100*	*99.95*	*50*
	Niobium (Nb)	*100*	*99.5*	*45*

Plate Preparation and Plaque Isolation

One tube containing 3 mL of tryptone soy soft that was placed into a water bath and maintained at 45^{o}C to avoid the agar from solidifying was prepared. 300µL of nutrient broth was added a sterile tube and mixed with 50µL of calcium chloride, followed by 1000µL of phage sample and 100µL of *E. anophelis*. The cultured tube was incubated for 30 minutes at 37^{o}C. Next, 3 mL of tryptone soy soft agar was poured into the tube containing the culture that had been incubated for 30 minutes in 37^{o}C and gently tapped. Subsequently, the soft agar was poured onto a tryptone soy hard agar plate and left to solidify. Once solidified, the plate was sealed with parafilm seal matrix and incubated at 37^{o}C for 24 hours. The plate was labelled accordingly. Following the 24-hour incubation at 37 ^{o}C, clear zones known as plaques were visually observed visually. Plaques were then eluted into a phage buffer that had been prepared manually and stored in the dark at 4^{o}C [17].

Agar Disc Diffusion for Antibacterial Activity Testing

A sterile cotton swab with 0.5 McFarland standard concentration of bacteria was swabbed on the surface of the nutrient agar plate. A 10µL of each type of metal was added to the 6mm discs, and the disc was left out to dry and was introduced onto the surface of the agar plate. The plate was then incubated for 24 hours in 37^{o}C in an inverted position. After the incubation, the antimicrobial activity was observed using HD Trinocular Stereo measuring the diameter from the edge of the 6mm (10µL) disc to the end three positions of the clear zone of inhibition the metal powders by using Image j. Each of the seven metal powders was performed in triplicates, and the results were attained in a graph.

Determination of the Minimal Inhibitory Concentration (MIC)

The minimal inhibitory concentration (MIC) is the lowest concentration of each alloy metal that inhibited the growth of the bacteria but does not necessarily kill them after 24 hours of incubation at 37^{o}C. Two-fold serial dilutions of the seven alloy metals were prepared on the 95-well microplates with a concentration ranging between ½ and 1/64. The logarithmic-phase development was accustomed to the bacterial suspension following turbidity of a 0.5 McFarland standard, yielding approximately 10^8 CFU/mL. Next, 7.5µL of bacteria was added in each well and the microplates were incubated for 24 hours at 37^{o}C. After incubation, each well was observed for their turbidity and was compared to the control. Nutrient broth filled with bacterial suspension without alloy metals was considered the positive control whereas the negative control was nutrient broth only [18].

Determination of the Minimum Bactericidal Concentration (MBC)

The minimum bactericidal concentration is the lowest concentration of alloy metals showing bactericidal activity that kills bacteria *in vitro*. A sterile loopful of broth from each MIC well was streaked in a zigzag form on the surface of the nutrient agar. After incubation, the MBC plates were observed for the growth of bacteria colony for each dilution subculture. If no noticeable development happened, the alloy metals at that specific dilution is assumed to be bactericidal. On the contrary, if there is a presence of growth, the antimicrobial properties of that specific alloy metal at that dilution were deemed bacteriostatic but not bactericidal [19].

Determination of the Synergistic Effects of the Combination of Phage and Seven Different Alloy Metals

The minimum Bactericidal concentration is the lowest concentration of metal powders lethal to the target bacteria in vitro. From each well from the MICs, a loopful of the broth was streaked in the zigzag form on the nutrient agar surface by using the sterile inoculation loop. The dilution of the subculture MIC well was recorded on each plate, and the plate was incubated for 24 hours at 37^{o}C. After incubation, the MBC plates were examined for colony growth or any lack of growth for each dilution subculture. If there was no visible growth, the metal powders were considered bactericidal at that dilution. On the contrary, if there was growth, the antibiotic was deemed bacteriostatic but not bactericidal at an inevitable dilution [19].

Results and Discussions

There a not much of information available about the nutrient requirements for *Elizabethkingia anophelis.* Good growth was observed (Figure 1) on Trypton Soy Agar (TSA) and Nutrient Agar (NA) at 37 °C. In NA, colonies were creamish-white, circular, smooth, raised elevations, and opaque with entire edges, however, in TSA the colonies were bigger in size, yellowish, circular, smooth, raised elevations and opaque with entire edges.

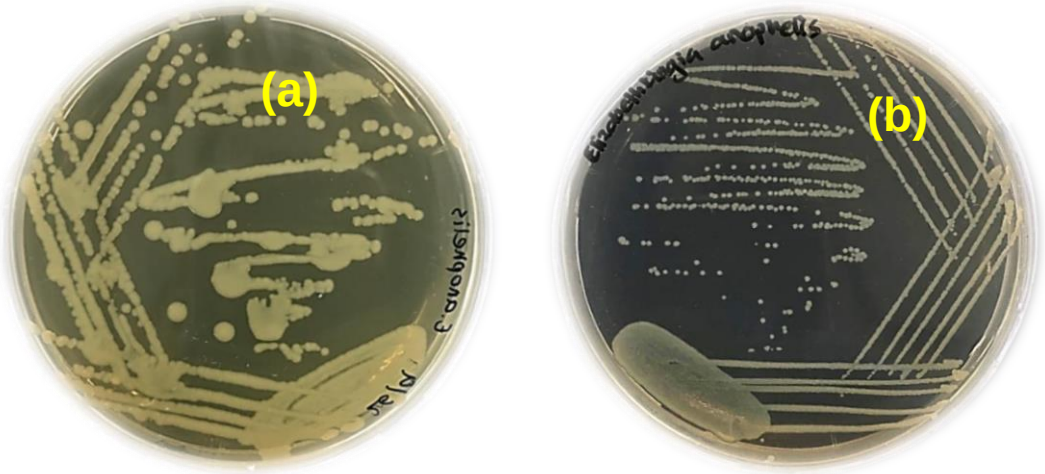

Figure 1. Culture of *Elizabethkingia anophelis* after 24 hours of incubation at 37^{o}C on (a) TSA, (b) NA.

Phage assay

Results revealed that there are specific phages infecting *E. anophelis* which were generally visualized as clear zones and irregular plaque (Figure 2). As seen in the Figure 1, the size of the plaques differed in in diameter. The smallest ones had a diameter of 10 mm, while the biggest had a diameter of 28 mm. Previous studies have shown that phage with a larger head (larger fraction of myophages) tends to form smaller plaques compared to a phage with a smaller head (large fraction of siphophages and podophages), which could be due to larger virions diffusing gradually and slowly through the top agar layer compared to the smaller phages, thus resulting in smaller plaques [20].

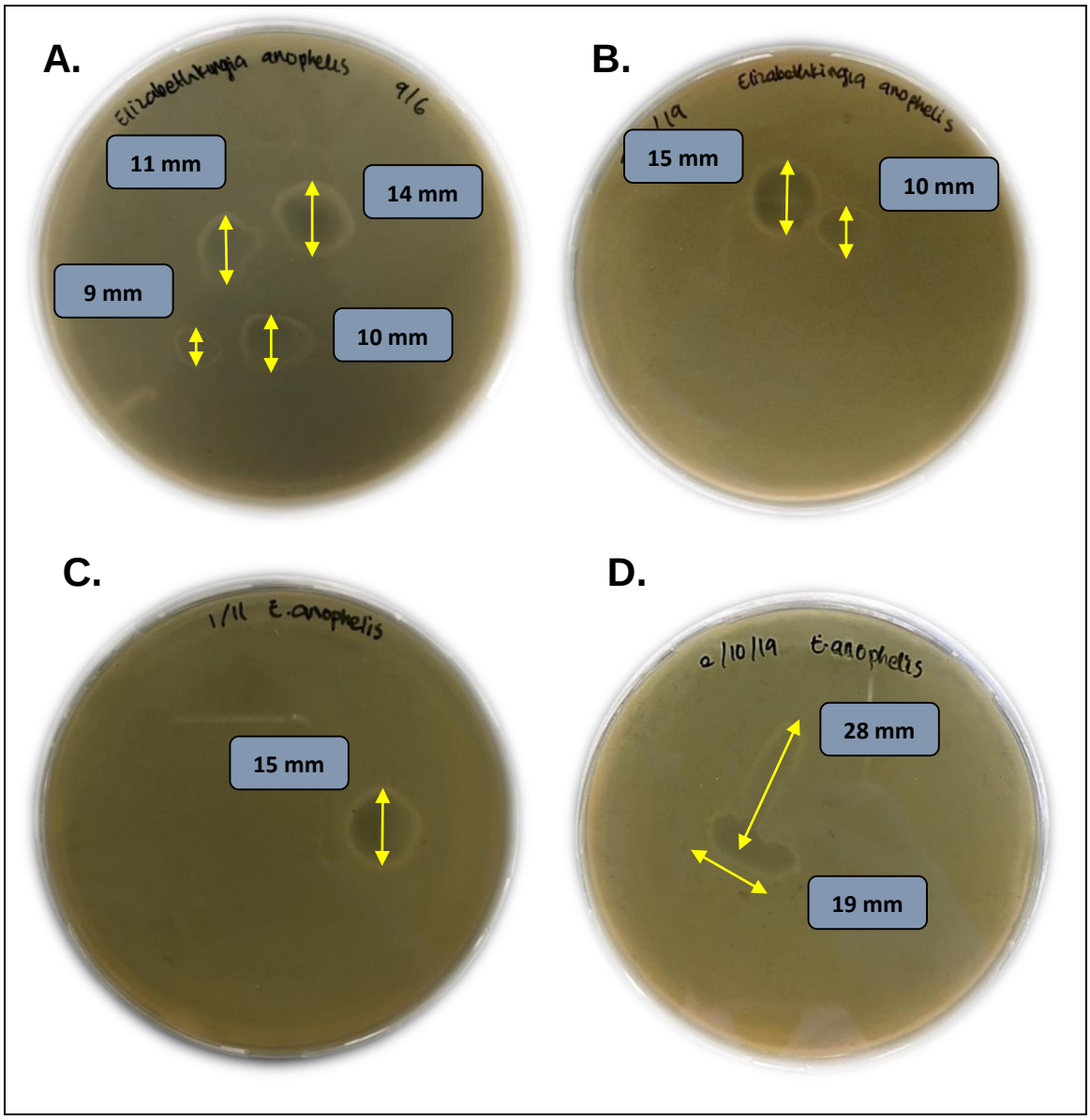

Figure 2. Plaque assay performed in quadruplets for (A), (B), (C) and (D). Results were shown after 24 hours of incubation at 37°C.

The plaque formation characteristic includes a clear plaque, irregular plaque, and turbid plaque at the edge. The clear plaques formed due to the *E.anophelis* is utterly susceptible to the phage on a bacterial lawn of a targeted bacteria. This clear plaque formation is usually due to lytic (virulent phages) [21]. Some of the plaques show slightly turbid at the edge because the cell at the edge of the plaque is not fully lysed [21]. Based on Jurczak-Kurek et al., (2016), this is due to the phage having integrated its nucleic acid into the host's genome and made its resistance to further infection from the phage. The integrated prophage DNA is replicated as part of the host DNA, and the phage does not lysis the host. Hence plaque appears turbid due to cell contain lysogenic phage.

Furthermore, the irregular plaque observed due to the plaque fused, and a higher number of phage concentration in bacteria host replicate which cause faster lysis of the bacteria

[22]. Many factors may affect plaque formation. One aspect is temperature, which may cause a significant effect on the host, virus, and interaction. Phage can't be expected to propagate throughout the temperature range that permits host growth [23]. Furthermore, the adsorption rate of plaque is also one of the affecting factors. The adsorption rate effect is usually on the plaque productivity, size and phage concentration on the plaque. The present of Stf significantly increases the phage adsorption rate [24].

Furthermore, the agar concentration is also one of the factors affecting the development of plaque. When the agar content is higher in the agar layer, the bacteriophage will take longer to diffuse to form a plaque [25]. Furthermore, the diffusion of phage across the agar may be wider due to the higher number of adhering bacteriophage and infecting a bacterium that presents a higher number of host cell receptors [26]. This has been supported by another earlier study [27] which demonstrated that when phage D4 and *Mycobacterium avium* subsp. *Paratuberculosis* (MAP) was observed when 2mM calcium chloride was present, the plaque formation was increase compare to 1mM calcium chloride.

Based on the inhibition zone analysis in Figure 3 (a-g), it was found that the following sequence from the highest to the lowest inhibition zone; Ti_{57}-Ta_{43}>Ti>GO>Ta>Nb>Ag> Ti_{55}-Ta_{43}-Ag_2.

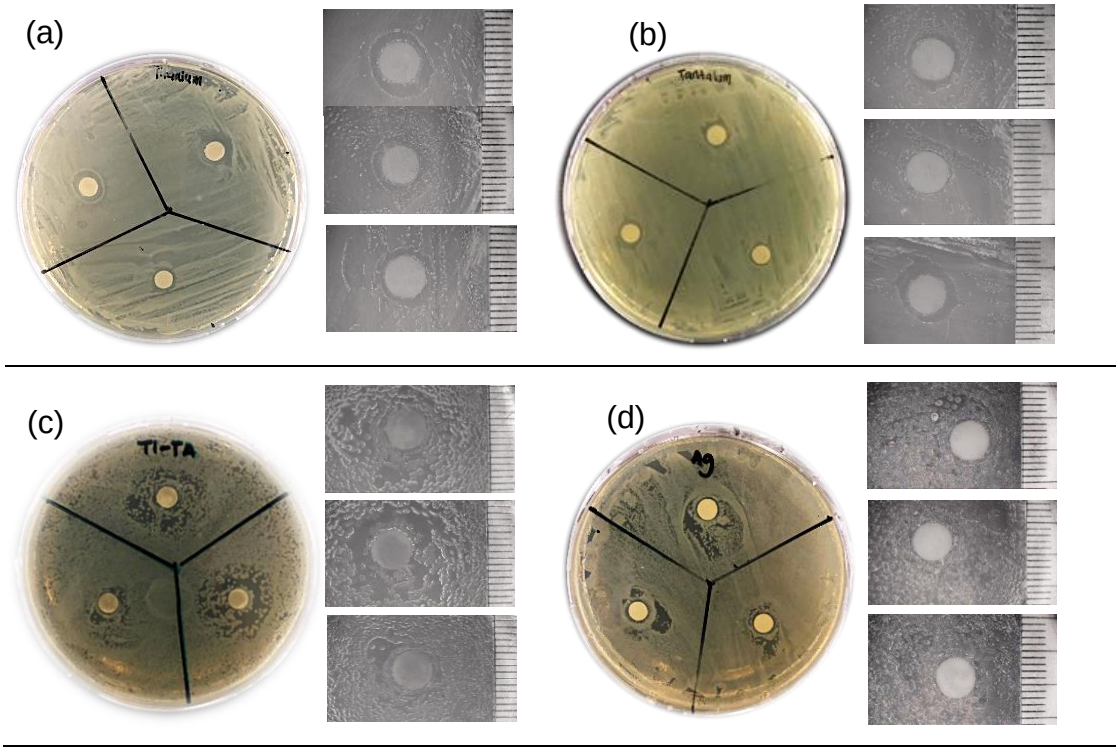

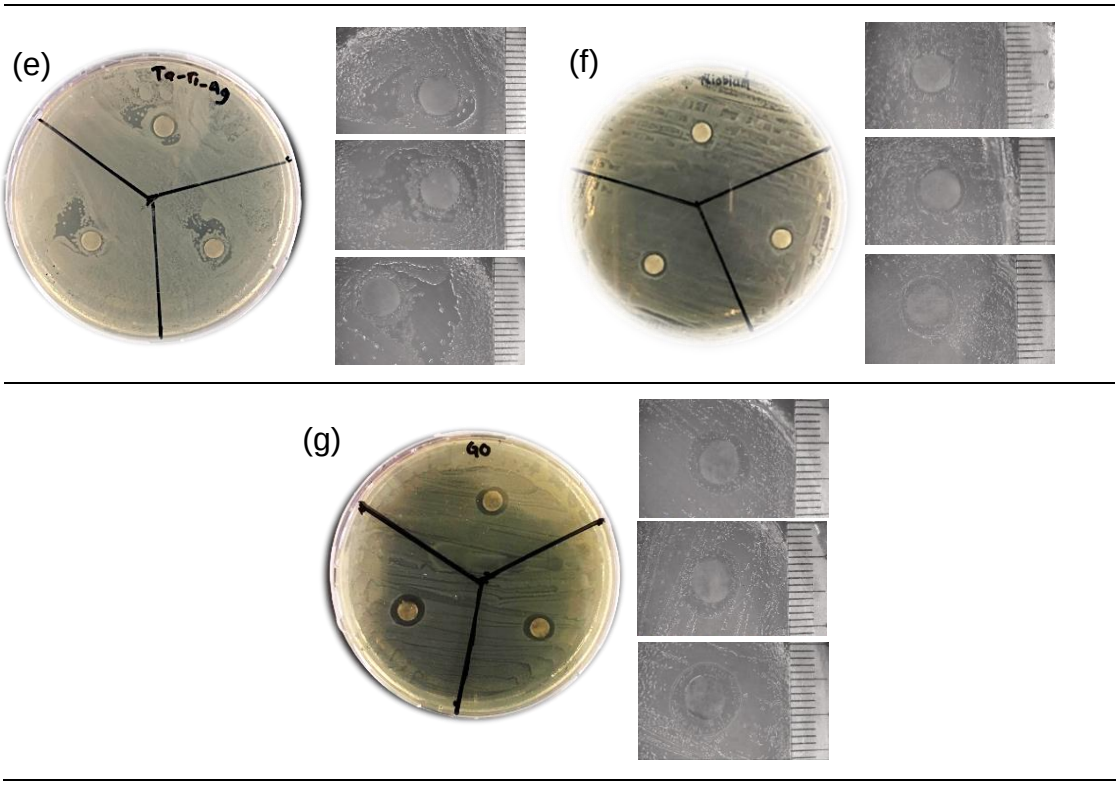

Figure 3. Inhibition Zone of different metal powders (200mg/mL): (a) Ti, (b) Ta, (c) Ti57-Ta43, (d) Ag, (e) Ti55-Ta43-Ag2, (f) Nb, and (g) GO against *E. anophelis*

The titanium (Ti) has the second-highest inhibition zone, which is 12±2.62 mm (Table 2), as displayed in Figure 3a. Previous study show, titanium has shown effective inhibiting the growth of *S. salivarious, S. mutans* [28] *S. aureus, B. subtilis* and *E. coli* [29]. Since *E. anophelis* can produce a biofilm, there has been evidence supports H_2O_2 and titanium biofilm interfaces resulting in the destruction of the bacteria within the biofilm. It has also been reported that the amount of H_2O_2 generated on titanium particles has achieved antibacterial activity against various bacterial species [30].

Although Tantalum as the individual element has shown an inhibition zone diameter of 10.33±1.52 mm (Figure 3b), even though, the potential activity of Ta has been studied extensively [31], it was found that the Ta did not display any intrinsic antibacterial activity or ability to inhibit biofilm formation against *S. aureus* and *S. epidermis* compared with the titanium [31]. However, some of the studies show that Ta_2O_5 reduces the number of *E. coli* its does not completely inhibit the growth. Its demonstrated that Ta ions might react with negatively charged cell wall on *E.coli* and initiate wall leakage, leading to bacteria's death [32]. According to Figure 3c, it was shown that the Ti_{57}-Ta_{43} has the highest antimicrobial properties toward *E. anophelis* compared with other metals. Some of the metal powders have the most remarkable antimicrobial efficacy when combined than pure Titanium, Tantalum or Silver. Due to their lower elastic modulus, increase corrosion resistance, and higher strength Ti_{57}-Ta_{43} are suitable for biomedical applications than pure Ti [33].

With the same following perspective, the Ag as a third element addition to TiTa all as Ti_{55}-Ta_{43}-Ag_2, the inhibition diameter against *E. anophelis* perceived to be around 8.66±0.57 mm (Table 2), as shown in Figure 3d and e. Studies [34, 35] revealed that AgNPs effective in killing both gram-positive and gram-negative strain of bacteria. Nevertheless, AgNPs are

practical and highly effective in destroying in gram-negative instead of gram-positive. This is could be due to their peptidoglycan layer [36]. Another study reports [37] that the smaller nanoparticles have greater antimicrobial activity and increase stability than larger nanoparticles. This could be due to the larger nanoparticle surface area, which gives a higher interaction area and ascending intracellular penetration. Silver nanoparticles have been shown to inhibit biofilm-forming bacteria's growth (*Serratia fonticola* and *Pantoea sp.)*[37].

Likewise, the Niobium inhibition zone (see in Figure 3f) was displayed diameter protection about 9.33±0.57 mm (Table 2), and according to Vaidya et al. 2019 [38], the introduction of niobium to copper (3.8%) has been demonstrated to reduce the bacterial count against *Escherichia coli* by up to 99% using viable bacterial count test. Studies have also demonstrated the bactericidal effect on *k.pneumoniae*, *A.baumannii*, and *E.faecium*. Based on Rakesh et al., 2014 [39] niobium doped zinc oxide nanoparticles that have been synthesized have also shown to have an effective bactericide towards *Escherichia coli, Xabthonobas oryzae, Salmonella typhii, Enterobacter aerogens*, and P*seudomonas aregunosa.*

Graphene Oxide (Figure 3g) has the third-highest inhibition zone within the inhibition diameter of 11.00±1.00 mm. The latest study showed that GO had been reported to exhibit storing antibacterial activity toward both Gram-negative and Gram-positive bacteria. It has been shown that it has a strong against *S. aureus* in graphene structure than *E. coli. This* is due to *E.coli* has a higher resistance against the direct interaction with the edge of the nano-walls [40]. However, the development of the antimicrobial activity can cause a physical interaction on the GO nanosheets' sharp edges and result in damaging the cell membrane. Furthermore, the chemical damage is initiated by the formation of ROS and charger transfer, subsequently resulting in oxidative stress. The stress on the membrane can induce fragmentation of genomic DNA and cell death [41].

Table 2. Antibacterial effect of alloy metals and phages in *Elizabethkingia anophelis.*

Alloy metals	Inhibition diameter (mm ± SD)	MIC (mg mL)	MBC (mg/mL)	Inhibition diameter (Alloy metals combination with phages) (mm ± SD)
Titanium	12.00±2.64	200	400	8.00±0.00
Tantalum	10.33±1.52	200	400	7.33±0.57
Titanium-Tantalum	20.00±5.19	100	400	7.00±0.00
Silver	8.66±0.57	50	100	7.33±0.57
Titanium-Tantalum-Silver	8.66±1.15	100	200	8.00±0.00
Graphene Oxide	11.00±1.00	25	50	9.33±0.57
Niobium	9.33±0.57	200	Neg	7.00±0.00

As for MIC and MBC in Figure 4, concentration plays a critical role in increasing the present study's antimicrobial activity. The Ti, Ta, Ti57-Ta43, Nb, Go, Ti55-Ta43-Ag2, and Ag at different concentrations determine their MIC values. The results exhibited that all the metal powders restrained the growth of the tested *E. anophelis* in the range of 6.25 to 400mg/mL. Furthermore, the available free metal ions in the medium may differ due to its composition [42]. When combined with silver, the Ti57-Ta43 was able to increase the inhibitory effect of

the TiTa MIC/MBC fractions in *E. anophelis*, in which consistent with a study by Garza-Cervantes et al., (2017).

It was also observed that all the studied metal powders except niobium exhibit an excellent antibacterial activity. Those had the lowest MBC and MIC indicate the highest antibacterial activity. Among the tested metal powders in this research, the Graphene Oxide shows the best antimicrobial activity within a MIC and MBC values of 6.25 and 50mh/ml, respectively. This is possibly due to the development of the antimicrobial activity by physical interaction sharp edges of the GO nanosheets damage cell membrane. Furthermore, the chemical damage is initiated by ROS and charger transfer, subsequently resulting in oxidative stress. The stress on the membrane can induce fragmentation of genomic DNA and cell death [41]. However, based on our study, niobium's antimicrobial efficacy was not significant in the MIC; however, the MBC tests show that there is still bacterial growth in 400mg/mL concentration.

Based on the result observation for a combination of phages and metal powders (Figure 5), shows there is a minor activity when metal powders and the phage are combined. The previous studies showed when the bacteriophages were contacted with metal, the number of bacteriophages reduced. It has also been demonstrated that copper and silver reduce different phages' growth [43]. One of the factors is also due to the order of the phage's exposure is revealed the fitness costs of sequential resistance. It also depends on the phage's timing [44].

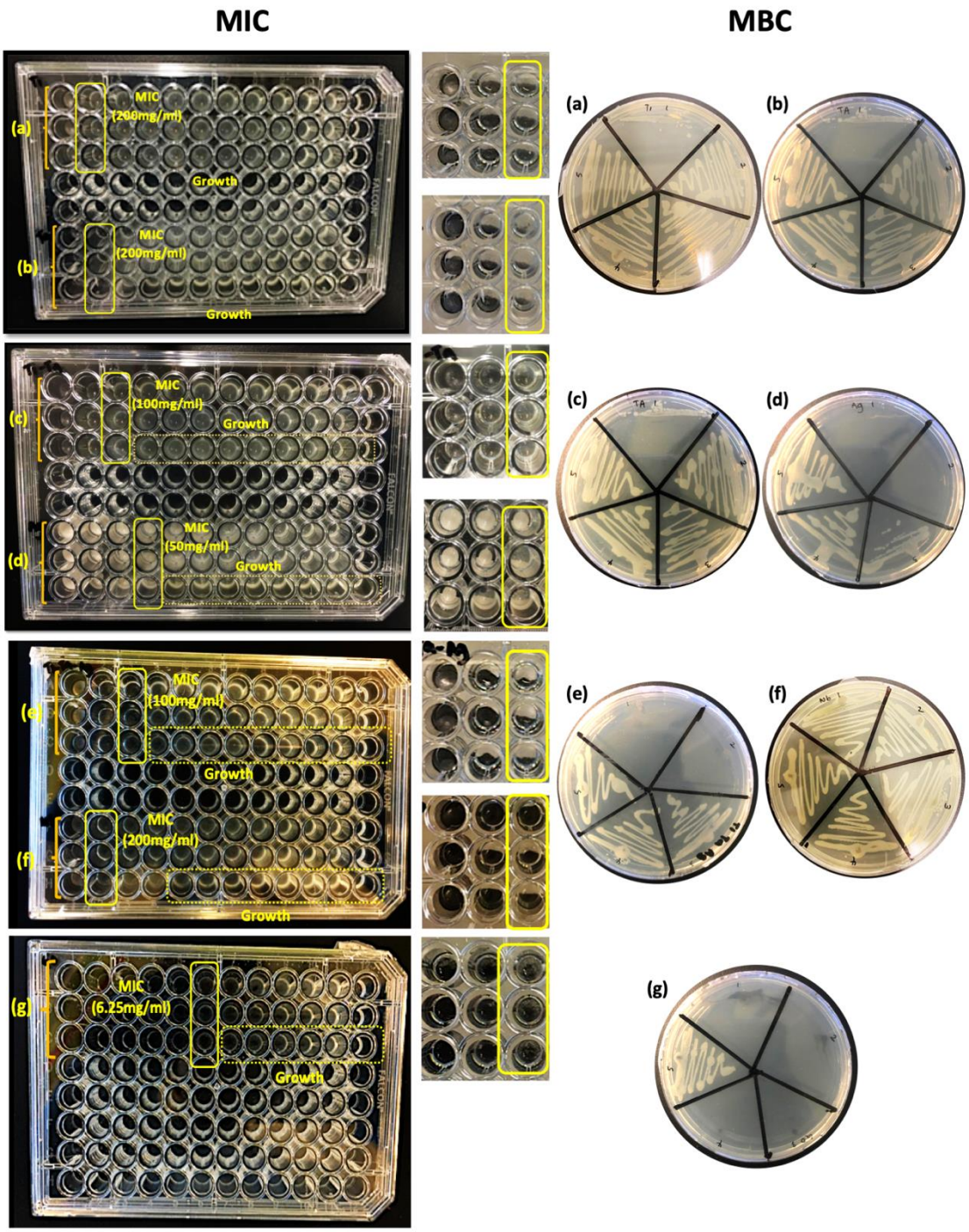

Figure 4. MIC and MBC of metal powders against *E. anophelis*; (a) Ti, (b) Ta, (c) Ti57-Ta43, (d) Ag, (e) Ti55-Ta43-Ag2, (f) Nb, and (g) GO

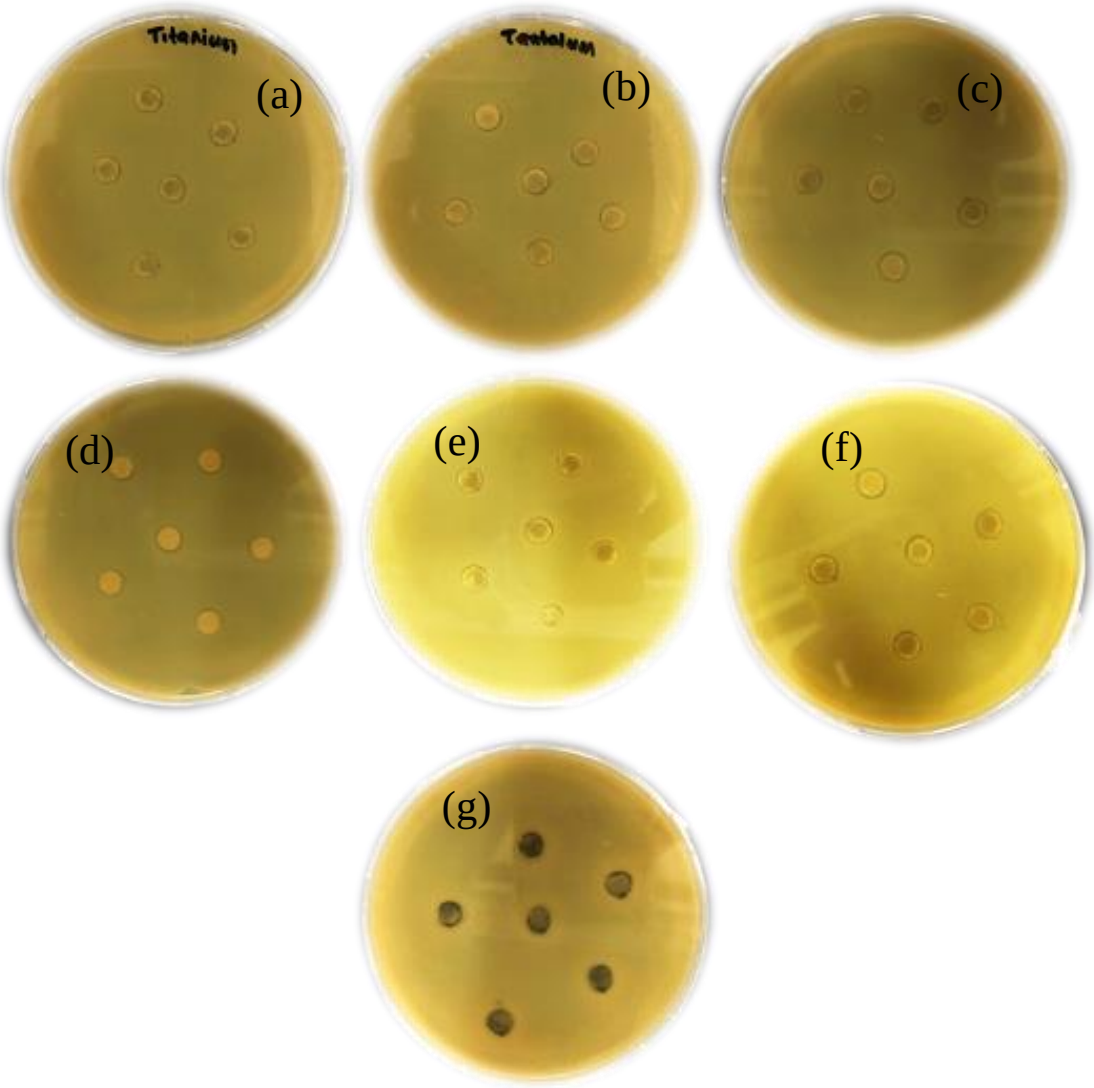

Figure 5: Inhibition zone of phages and combination of different metal powders: (a) Ti, (b) Ta, (c) Ti57-Ta43, (d) Ag, (e) Ti55-Ta43-Ag2, (f) Nb, and (g) GO against *E. anophelis.*

Conclusion

As a conclusion, the combination of the alloy metals and nanoparticles showed no significant activity. *E. anophelis* was able to be infected by plaque forming phages from the sewage water and alloy metals showed significant activity against *E. anophelis.* Hence, these findings conclude that both phage and alloy metals are better used independently.

At this point, additional studies should be done to gain a better understanding of the biological properties of bacteriophages and the antimicrobial properties of the alloy metals, along with the mechanisms involved in phage combined with alloy metals in bacterial host interaction. Despite the knowledge of their manipulation *in-vitro*, understanding of their behaviour *in-vivo* is limited, particularly in clinical trials. Future studies on *in-vivo* are certainly called for. This study is important to address and provide an alternative approach to one of the world's top global health threats, which is antibiotic resistance. Nevertheless, the encouraging results obtained so far suggest that the continued experimentation with phage/metals combinations is an endeavour, which likely will pay off in future as an ultimate and robust

remedy against multi-drug resistant bacteria.

Acknowledgement

Authors would also like to express their sincere appreciation to Management and Science University for providing for providing the Seed Grant (SG-010-012019-FHLS) to conduct this research.

Author Contributions

D.G.D., A.Z. and S.N.S. contributed substantially to the conception and design of the study, the acquisition of data, or the analysis and interpretation. All authors participated in the writing of the article.

Disclosure of Conflict of Interest

The authors declare that they have no competing interests.

Compliance with Ethical Standards

This study was granted approval (MSU-RMC-02/FR01/02/L1/046) by Human Ethical Committed of the Management & Science University, Shah Alam, Selangor State, Malaysia.

References

1. Janda, J.M. and D.L. Lopez, *Mini review: new pathogen profiles: Elizabethkingia anophelis.* Diagnostic microbiology and infectious disease, 2017. **88**(2): p. 201-205.
2. Kämpfer, P., et al., *Elizabethkingia anophelis sp. nov., isolated from the midgut of the mosquito Anopheles gambiae.* International journal of systematic and evolutionary microbiology, 2011. **61**(11): p. 2670-2675.
3. Wang, M., et al., *The antibiotic resistance and pathogenicity of a multidrug-resistant Elizabethkingia anophelis isolate.* MicrobiologyOpen, 2019. **8**(11): p. e804.
4. Perrin, A., et al., *Evolutionary dynamics and genomic features of the Elizabethkingia anophelis 2015 to 2016 Wisconsin outbreak strain.* Nature communications, 2017. **8**: p. 15483.
5. Lau, S.K., et al., *Evidence for Elizabethkingia anophelis transmission from mother to infant, Hong Kong.* Emerging infectious diseases, 2015. **21**(2): p. 232.
6. Lin, J.-N., et al., *Genomic features, phylogenetic relationships, and comparative genomics of Elizabethkingia anophelis strain EM361-97 isolated in Taiwan.* Scientific reports, 2017. **7**(1): p. 1-8.
7. Chew, K.L., et al., *Elizabethkingia anophelis is the dominant Elizabethkingia species found in blood cultures in Singapore.* Journal of clinical microbiology, 2018. **56**(3).
8. Coyle, A.L., *Elizabethkingia anophelis: exploring the outbreak of disease in the Midwest.* Nursing2019, 2017. **47**(3): p. 61-63.
9. Nielsen, H.L., et al., *Rare Elizabethkingia anophelis meningitis case in a Danish male.* JMM case reports, 2018. **5**(8).
10. Hassan, W.M.N.W., et al., *An uncommon Elizabethkingia meningoseptica septicemia in hemorrhagic stroke with septic shock patient during prolonged neuro-intensive care management.* Anaesthesia, Pain & Intensive Care, 2019: p. 268-271.
11. Phoon, H.Y., et al., *Distribution, genetic diversity and antimicrobial resistance of*

clinically important bacteria from the environment of a tertiary hospital in Malaysia. Journal of global antimicrobial resistance, 2018. **14**: p. 132-140.
12. Ransangan, J., et al., *Identification of Elizabethkingia meningoseptica from American bullfrog (Rana catesbeiana) farmed in Sabah, Malaysia using PCR method and future management of outbreak.* Malaysian Journal of Microbiology, 2013. **9**(1): p. 13-23.
13. Jian, M.-J., et al., *Multicentre MDR Elizabethkingia anophelis isolates: Novel random amplified polymorphic DNA with capillary electrophoresis systems to rapid molecular typing compared to genomic epidemiology analysis.* Scientific reports, 2019. **9**(1): p. 1-10.
14. Papp-Wallace, K.M., et al., *Carbapenems: past, present, and future.* Antimicrobial agents and chemotherapy, 2011. **55**(11): p. 4943-4960.
15. Frank, T., et al., *First case of Elizabethkingia anophelis meningitis in the Central African Republic.* The Lancet, 2013. **381**(9880): p. 1876.
16. Azman, N.R. and A. Zajmi, *Fusobacterium ulcerans phage isolation from the environmental sample.* Journal of Management & Science, 2017. **15**(2).
17. Kropinski, A.M., et al., *Enumeration of bacteriophages by double agar overlay plaque assay*, in *Bacteriophages*. 2009, Springer. p. 69-76.
18. Zajmi, A., et al., *Ultrastructural study on the antibacterial activity of artonin e versus streptomycin against Staphylococcus aureus strains.* PLoS One, 2015. **10**(6): p. e0128157.
19. Zulkiffly, M.F. and A. Zajmi, *Investigation of potential antibacterial activity of Salvadora persica in combination with Mentha arvensis against Staphyloccocus SPP.* International Journal of Medical Toxicology & Legal Medicine, 2018. **21**(3and4): p. 288-292.
20. Jurczak-Kurek, A., et al., *Biodiversity of bacteriophages: morphological and biological properties of a large group of phages isolated from urban sewage.* Scientific reports, 2016. **6**(1): p. 1-17.
21. Abedon, S., *Detection of bacteriophages: Phage plaques.* Bacteriophages: Biology, Technology, Therapy; Harper, DR, Abedon, ST, Burrowes, BH, McConville, M., Eds, 2018.
22. Francis, F., R. Miller, and M. Nagra, *Phage overlay assay for quantification of infectious bacteriophage particles.* JEMI Meth, 2017. **1**: p. 18-21.
23. Tokman, J.I., et al., *Temperature significantly affects the plaquing and adsorption efficiencies of Listeria phages.* Frontiers in microbiology, 2016. **7**: p. 631.
24. Gallet, R., S. Kannoly, and N. Wang, *Effects of bacteriophage traits on plaque formation.* BMC microbiology, 2011. **11**(1): p. 1-16.
25. Abedon, S.T. and T.I. Katsaounis, *Basic phage mathematics*, in *Bacteriophages*. 2018, Springer. p. 3-30.
26. Choi, C., et al., *The effect of cell size on the burst size of T4 bacteriophage infections of Escherichia coli B23.* J Exp Microbiol Immunol, 2010. **14**: p. 85-91.
27. Foddai, A., C.T. Elliott, and I.R. Grant, *Optimization of a phage amplification assay to permit accurate enumeration of viable Mycobacterium avium subsp. paratuberculosis cells.* Applied and Environmental Microbiology, 2009. **75**(12): p. 3896-3902.
28. Petrini, P., et al., *Antibacterial activity of zinc modified titanium oxide surface.* The International journal of artificial organs, 2006. **29**(4): p. 434-442.
29. Eshghinejad, P., et al., *Electrophoretic deposition of bioglass/graphene oxide composite on Ti-alloy implants for improved antibacterial and cytocompatible properties.* Materials Technology, 2020. **35**(2): p. 69-74.
30. Santhoshkumar, T., et al., *Green synthesis of titanium dioxide nanoparticles using Psidium guajava extract and its antibacterial and antioxidant properties.* Asian Pacific

journal of tropical medicine, 2014. **7**(12): p. 968-976.
31. Harrison, P., et al., *Does tantalum exhibit any intrinsic antimicrobial or antibiofilm properties?* The bone & joint journal, 2017. **99**(9): p. 1153-1156.
32. Szunerits, S. and R. Boukherroub, *Antibacterial activity of graphene-based materials.* Journal of Materials Chemistry B, 2016. **4**(43): p. 6892-6912.
33. Zhou, Y.-L., et al., *Comparison of various properties between titanium-tantalum alloy and pure titanium for biomedical applications.* Materials transactions, 2007. **48**(3): p. 380-384.
34. Benyettou, F., et al., *Synthesis of silver nanoparticles for the dual delivery of doxorubicin and alendronate to cancer cells.* Journal of Materials Chemistry B, 2015. **3**(36): p. 7237-7245.
35. Kędziora, A., et al., *Similarities and differences between silver ions and silver in nanoforms as antibacterial agents.* International journal of molecular sciences, 2018. **19**(2): p. 444.
36. Slavin, Y.N., et al., *Metal nanoparticles: understanding the mechanisms behind antibacterial activity.* Journal of nanobiotechnology, 2017. **15**(1): p. 1-20.
37. Gurunathan, S., et al., *Enhanced antibacterial and anti-biofilm activities of silver nanoparticles against Gram-negative and Gram-positive bacteria.* Nanoscale research letters, 2014. **9**(1): p. 1-17.
38. Vaidya, M., et al., *Single and combined antimicrobial efficacies for nine metal ion solutions against Klebsiella pneumoniae, Acinetobacter baumannii and Enterococcus faecium.* International Biodeterioration & Biodegradation, 2019. **141**: p. 39-43.
39. Rakesh, S.A. and M. Netkal, *Made Gowda, Kithanakere Ramesh Raksha, Synthesis of niobium doped ZnO nanoparticles by electrochemical method: characterization, photodegradation of indigo carmine dye and antibacterial study.* Adv. Nanopart, 2014. **3**: p. 133-147.
40. Chowdhuri, A.R., et al., *A ZnO decorated chitosan–graphene oxide nanocomposite shows significantly enhanced antimicrobial activity with ROS generation.* RSC Advances, 2015. **5**(61): p. 49420-49428.
41. Anand, A., et al., *Graphene oxide and carbon dots as broad-spectrum antimicrobial agents–a minireview.* Nanoscale horizons, 2019. **4**(1): p. 117-137.
42. Garza-Cervantes, J.A., et al., *Synergistic antimicrobial effects of silver/transition-metal combinatorial treatments.* Scientific reports, 2017. **7**(1): p. 1-16.
43. Versoza, M., et al., *Reduction of Escherichia Coli Using Metal Plates with the Influenced of Applied Low Current and Physical Barrier of Filter Layers.* International Journal of Environmental Research and Public Health, 2019. **16**(20): p. 3887.
44. Wright, R.C., et al., *Resistance evolution against phage combinations depends on the timing and order of exposure.* MBio, 2019. **10**(5): p. e01652-19.